Available online at www.sciencedirect.com
SCIENCE DIRECT®
Journal of Magnetic Resonance 177 (2005) 203–211
JMR Journal of Magnetic Resonance
www.elsevier.com/locate/jmr

Improving pulse sequences for 3D DOSY: Convection compensation

Mathias Nilsson *, Gareth A. Morris

School of Chemistry, University of Manchester, Oxford Road, Manchester M13 9PL, UK

Received 8 June 2005; revised 21 July 2005
Available online 2 September 2005

Abstract

Signal overlap in the NMR dimension significantly complicates the construction and analysis of 2D diffusion-ordered (DOSY) spectra. Such problems can often be reduced or even eliminated by extending the NMR domain of a DOSY experiment into two dimensions, giving a 3D-DOSY spectrum. To date such experiments have generally sacrificed some signal-to-noise ratio and have required extensive and time-consuming phase cycling. A new family of pulse sequences with internal diffusion encoding (IDOSY) has been introduced which avoids both of these problems. It is often straightforward to incorporate convection compensation in such sequences at no cost in signal-to-noise ratio. Here, some of the problems caused by convection in DOSY are described and illustrated, and the efficacy of convection compensation in the 2DJ-IDOSY and COSY-IDOSY experiments is demonstrated.

Keywords: DOSY; Diffusion; Convection; Pulsed field gradients; 3D DOSY

1. Introduction

Diffusion-ordered spectroscopy seeks to separate the NMR signals of components in a mixture on the basis of their apparent diffusion coefficients [1–3]. The signal amplitude in a pulse field gradient spin echo (PFGSE) or pulse field gradient stimulated echo (PFGSTE) experiment can be generally expressed as

$$S = S_0 e^{-D\gamma^2\delta^2 g^2 \Delta'}, \quad (1)$$

where S is the signal amplitude, S_0 is the signal amplitude in the absence of field gradients, D is the diffusion coefficient, γ is the magnetogyric ratio, δ is the gradient pulse width, g is the gradient amplitude, and Δ' is the diffusion time corrected for the effects of finite gradient pulse width. In a prototypical DOSY experiment, a series of spectra recorded at different gradient amplitudes is collected, and peak amplitudes are fitted to Eq. (1). The 1D spectrum is then extended into a second, diffusion, dimension with Gaussian lineshapes centred on the calculated diffusion coefficient (D) and with linewidths determined by the estimated error of the fitting.

In high resolution (HR)-DOSY [4] the decays are fitted to a monoexponential curve, and differences in apparent diffusion coefficient as small as 0.5% can be distinguished in well-resolved spectra. As, however, overlap is common in NMR spectra and resolving superimposed exponentials is notoriously hard [5], a number of methods to resolve spectra into components with different rates of diffusion have emerged. These can roughly be divided into single channel [6–8] and multi channel [9–14] methods. In single channel methods the decay of each peak (or data point) is analysed without reference to the rest of the data; resolution of superimposed exponentials is accomplished by some approximation to the inverse Laplace transform, for example biexponential fitting, or the SPLMOD [8], CONTIN [8] or MAXENT [7] algorithms. In multichannel methods, the whole, or whole sections of, spectra are used simultaneously to extract pure component spectra and determine diffusion coefficients, using various assumptions as to the number of components and/or the exact form of the decays; such methods include DE-

* Corresponding author. Fax: +44 161 275 4598.
E-mail address: mathias.nilsson@manchester.ac.uk (M. Nilsson).

1090-7807/$ - see front matter © 2005 Elsevier Inc. All rights reserved.
doi:10.1016/j.jmr.2005.07.019

CRA [14], CORE [12], and MCR [13]. Neither the single channel nor the multichannel methods have been shown to be able to resolve superimposed signals with similar diffusion coefficients. If monoexponential fitting (HR-DOSY) is applied to overlapping signals, the apparent diffusion coefficient will be a compromise value, which can complicate the analysis of the DOSY spectra significantly.

As high resolution in the diffusion dimension is only available for signals which are well-separated in the frequency domain, the idea of extending the 2D-DOSY experiment into higher dimensionality is a logical development. Many 3D-DOSY experiments have been devised [15–25]; a new family of such experiments has recently been proposed, in which diffusion encoding is incorporated into pre-existing delays in conventional 2D pulse sequences [20–22]. Such experiments lend themselves particularly readily to compensation for one of the most serious complications of DOSY, convection.

2. Convection

Because the mean square displacement of a diffusing particle scales according to the square root of time, NMR pulse sequences designed to measure diffusion can be exquisitely sensitive to the confounding effects of coherent motion, which scales linearly with time. Physical movements of the sample tube and/or pulsed field gradient coil can cause significant difficulties in diffusion measurements [26], but one of the commonest and most troublesome sources of coherent sample motion is thermal (Rayleigh–Bénard) convection.

When the liquid at the base of an NMR tube is warmer than that at the top, there is a tendency for the warmer, and hence less dense, liquid to rise to the top, where it cools and then returns to the bottom in a continuous cycle—the phenomenon of convection. (In practice, and perhaps counter-intuitively, convection can also occur with horizontal, as opposed to vertical, temperature gradients [27].) Ideally, convection only occurs when the temperature gradient exceeds a critical value, which depends in part on the sample geometry. In practice, the onset of convection is generally earlier than predicted by theory, and is influenced by horizontal as well as vertical temperature gradients.

In a typical DOSY experiment, a uniform sample flow velocity v introduces a phase modulation of the signal [28]:

$$S = S_0 e^{-D\gamma^2\delta^2 g^2 \Delta'} e^{i\gamma g v \delta \Delta}. \quad (2)$$

Representing convection by a crude model of equal and opposite flows each of uniform velocity leads to cancellation of the imaginary part of Eq. (2) and the result is a cosine modulation [29]:

$$S = S_0 e^{-D\gamma^2\delta^2 g^2 \Delta'} \cos(\gamma g v \delta \Delta). \quad (3)$$

In practice, convection in an NMR tube involves a (symmetric) spectrum of different flow rates which rapidly damps the cosine factor in Eq. (3), but the qualitative conclusion remains that convection causes an accelerated decay of the signal, and in severe cases inversion, of the signal. When convection is slow, the effect on diffusion measurements is to increase the apparent diffusion coefficients; faster convection can lead to more complex flow patterns [30] and to turbulence, and may cause the PFGSTE signal to disappear almost entirely.

In practice, a number of strategies can be used either to delay the onset of convection or to mitigate its effects. (a) Convection-compensated pulse sequences are the main subject of the present investigation and will be discussed in further detail below [28,31]. (b) Reducing the sample radius by using a smaller diameter sample tube [32,33] delays convection. (c) Reducing the sample height, for example by the use of a restricted sample volume (e.g., a Shigemi tube [34], with or without a central glass cylinder to constrain the liquid motion still further [35]), also delays convection. Unfortunately, the disturbance of main field homogeneity limits the value of this approach in high resolution NMR quite severely; in principle there are also concerns about restricted diffusion [34]. (d) Spinning the sample [36,37] changes the direction of the net force on a liquid voxel from the vertical, effectively changing the size and aspect ratio of the convection cell markedly, but this imposes stringent requirements on the transverse uniformity of the pulsed field gradient and the synchronization of the sample spinning with the gradient pulses. (e) Using transverse, rather than vertical, pulsed field gradients removes the sensitivity to vertical motion [28], but unfortunately convective motion in NMR sample tubes is not purely vertical [27,30] and transverse gradient probes are not widely available. (f) Using a more viscous solvent makes convection less likely, but is frequently not an acceptable chemical option. (g) The problem may be attacked at source by reducing the temperature gradient.

Sample temperature gradients can arise from a variety of causes, including radiofrequency heating [28], differential heating of the outside of the probe by shim coils, conduction along the sample tube etc., but by far the commonest source is the airflow (“variable temperature” or “VT” air or nitrogen gas) used to control the sample temperature. Most NMR probes use an airflow which starts at the bottom of the sample and flows upwards, although it has been reported that reversing the direction can reduce convection [32]. Clearly the effect here will depend on whether the sample is being heated or cooled, although experimentally it is observed that convection remains a problem whether the air supply is above or below the quiescent sample temperature. Increasing the flow rate of the VT air can make the

temperature more uniform and hence delay the onset of convection [32,38–40], but sample vibration limits the flow rates usable. Replacing the VT air flow with liquid [41], for example a polyfluorinated hydrocarbon, can greatly reduce temperature gradients but is not practical for routine work. A related expedient, using a coaxial capillary sample inside a normal NMR tube, either empty (to insulate the inner sample) or filled with an NMR-silent liquid (to improve thermal conduction along the sample), has met with some success [27,33]. Using sample tubes made out of sapphire, which has a much higher thermal conductivity than glass, is an attractive but expensive option.

3. Pulse sequences for convection-compensated 3D DOSY

Diffusion encoding can be added to virtually any nD NMR experiment, resulting in an $(n+1)$D-DOSY experiment. Recently, several pulse sequences where the diffusion encoding pulses are incorporated within the parent sequence (the IDOSY family) [20–22], have been described, utilizing the logic of a previous TOCSY-IDOSY sequence [16]. Previously, almost all 3D sequences had been constructed by concatenating a diffusion encoding sequence with the parent experiment in the form DOSY-X or X-DOSY [15,17–19,23–25,42]. Often this is a perfectly serviceable approach, but when the parent pulse sequence either includes or can accommodate a delay of the order of tens of milliseconds for diffusion, the IDOSY approach can both substantially decrease the need for phase cycling and increase the signal-to-noise ratio obtainable. Figs. 1A and C show pulse sequences for COSY-IDOSY [21] and 2DJ-IDOSY [20], respectively; the diffusion encoding is incorporated in the Hahn echo (or antiecho) and spin echo, respectively. In both cases the coherence transfer pathways are identical to those in the parent experiment. In the COSY-IDOSY and 2DJ-IDOSY experiments a reduction in minimum experimental time of 32 and four times, respectively, and an increase in signal-to-noise ratio of a factor 1.5–2.0 have been demonstrated.

The effect of linear flow during a typical DOSY pulse sequence is to introduce a velocity-dependent phase modulation of the form of Eq. (2). The phase errors arise because the spins encounter a steadily increasing or decreasing field gradient as they move, and hence fail to refocus fully in an echo. If, however, two successive echoes are performed, then the second echo can compensate for the phase error accumulated during the first, and the refocused signal becomes independent of flow. A very simple way to achieve this is with two successive gradient echoes of opposite polarity, so that the gradient pulse signs follow the sequence $+\,-\!-\,+$. If the pulse timings and amplitudes are identical in the two echoes (or adjusted to give identical effects [40], as for example to accommodate for solvent suppression in the CONVEX experiment [43]) then constant velocity flow phase errors cancel completely. Such a pulsed field gradient double gradient echo (PFGDGE) lends itself readily to insertion into pulse sequence delays as a flow-compensated diffusion weighting element.

The same principle of using two successive echoes may be applied to the pulsed field gradient stimulated echo, the type of pulse sequence most commonly used for DOSY, yielding the convection-compensated pulsed field gradient double stimulated echo (PFGDSTE) sequence [28,31]. Unfortunately each of the two stimulated echoes sacrifices 50% of the available signal, so this type of sequence incurs a significant sensitivity penalty. If PFGDGE convection compensation is applied during a spin or Hahn echo, however, there is no loss of signal-to-noise ratio compared to the uncompensated sequence, as has been noted for the INEPT-IDOSY and HMQC-IDOSY sequences [22]. In the 2DJ-IDOSY [20] and COSY-IDOSY [21] sequences, convection compensation can similarly be included at virtually no cost in sensitivity. A thorough treatment of the theory behind convection compensated pulse sequences has been given previously [28,40,44]. In the present investigation, convection compensation of the COSY-IDOSY and 2DJ-IDOSY experiments (Figs. 1B and D) is examined.

4. Experimental

Two samples were used in this investigation: sample 1 contained approximately 2% camphene, 2% quinine, and 10% geraniol (w/v) in $CDCl_3$, using tetramethylsilane (TMS) as a chemical shift reference, and sample 2 containing 0.5% glucose, 0.2% 1-propanol, and 0.25% ethanol (w/v) in D_2O, using sodium 3-(trimethylsilyl)-propionate-2,2,3,3-d_4 (TSP) as a chemical shift reference. The pulse sequences used for 3D DOSY in this investigation were COSY-IDOSY [21] with and without convection compensation (Figs. 1A and B) and 2DJ-IDOSY [20] with and without convection compensation (Figs. 1C and D). In addition to the IDOSY sequences, for 2D DOSY, the oneshot sequence [45] (Fig. 1E) and a slight variation (Fig. 1F) on the previously published convection compensated PFGDSTE sequence [28,31] were used.

All measurements were carried out non-spinning on a 400 MHz Varian Inova instrument, using a 5 mm diameter indirect detection probe equipped with a gradient coil allowing gradient pulses up to 30 G cm^{-1}. Unless otherwise stated, temperature control was used at 25 °C for sample 1 and 37 °C for sample 2, respectively, in a room air-conditioned at about 20 °C. All 2- and 3D-DOSY experiments were acquired with a

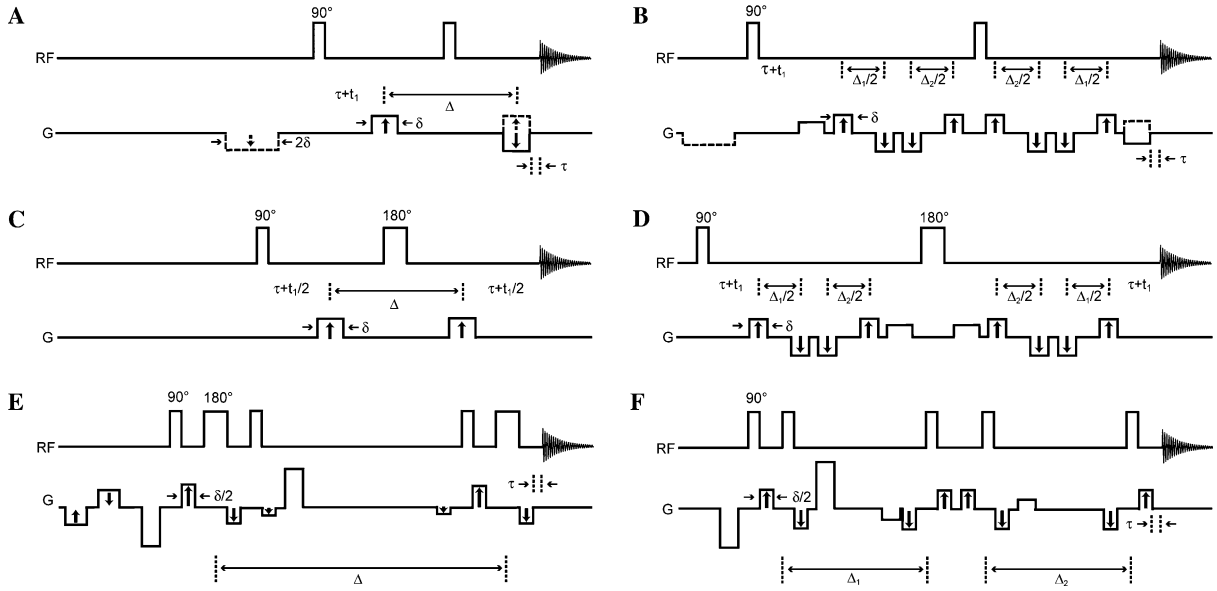

Fig. 1. Pulse sequences for 2D and 3D DOSY. (A) Standard COSY-IDOSY [21]; (B) convection compensated COSY-IDOSY; (C) standard 2DJ-IDOSY [20]; (D) convection compensated 2DJ-IDOSY; (E) oneshot [45] and (F) a convection compensated sequence using a pulsed field gradient double stimulated echo (PFGDSTE). The sequences show radio frequency (RF) and gradient (G) pulses, with vertical arrows indication the gradient amplitudes changed to vary the diffusion encoding; a delay τ is allowed for gradient stabilization after each gradient pulse.

diffusion delay (Δ) of 0.2 s for sample 1 and 0.3 s for sample 2; a diffusion-encoding pulse width (δ) of 2 ms; and gradient strengths, chosen to give equally spaced steps of gradient squared, ranging from of 3.0 to 27.3 G cm^{-1}. As previously described, the 2D [4] and 3D [15] DOSY displays were constructed by fitting the decay of each peak to the appropriate form of Eq. (1), assuming monoexponential decays [4]. For the 3D-DOSY experiments, cross-peaks were defined by manual selection of 2D integration regions; cross-peak volumes were corrected for baseplane noise by subtraction of the appropriate proportion of the integrated volume of a large sample of baseplane from an empty region of the spectrum [19].

For the oneshot sequence [45] (Fig. 1E), Δ' is equal to $\Delta + \delta(\alpha^2 - 2)/6 + \tau(\alpha^2 - 1)/2$, where α is the imbalance ratio of the bipolar pulse pairs and τ is the time between the midpoints of the individual gradient pulses in one diffusion encoding period; for the double stimulated echo (Fig. 1F), the standard COSY-IDOSY, and 2DJ-IDOSY $\Delta' = \Delta - \delta/3$, and for the convection compensated COSY-IDOSY and 2DJ-IDOSY $\Delta' = \Delta - 4\delta/3$. The data collected with the oneshot sequence used an imbalance factor (α) of 0.2 for the diffusion-encoding gradient pulses. For the 2D-DOSY experiments, 16,384 complex data points were acquired for each of 16 gradient amplitudes. For 2DJ-IDOSY experiments, 32 increments of 8192 complex data points, and for COSY-IDOSY 1024 increments of 2048 complex data points, were recorded for each of 8 gradient amplitudes. Sinebell weighting was applied in both dimensions before Fourier transformation.

5. Results and discussion

Fig. 2 shows how the amplitude of the quinine methyl signal in sample 1 varies with degree of diffusion delay imbalance ($\Delta_1 - \Delta_2$) in the pulse sequence of Fig. 1F for different temperatures. Since the two halves of the experiment together compensate for linear motion of the spins, any change in signal intensity as the two de-

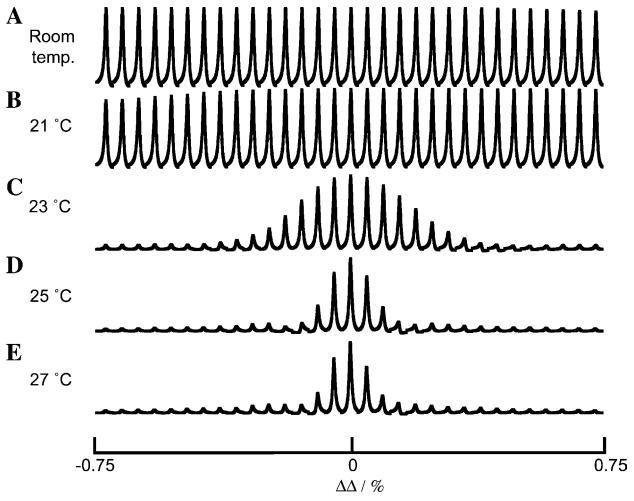

Fig. 2. Signal amplitudes from the quinine methyl peak at 3.9 ppm in sample 1 as acquired with the PFGDSTE sequence of Fig. 1F, varying the imbalance between the two diffusion delays ($\Delta\Delta = \Delta_1 - \Delta_2$) at different temperatures. (A) No temperature control (approximately 20 °C); (B) temperature controlled at 21 °C; (C) temperature controlled at 23 °C; (D) temperature controlled at 25 °C; (E) temperature controlled at 27 °C.

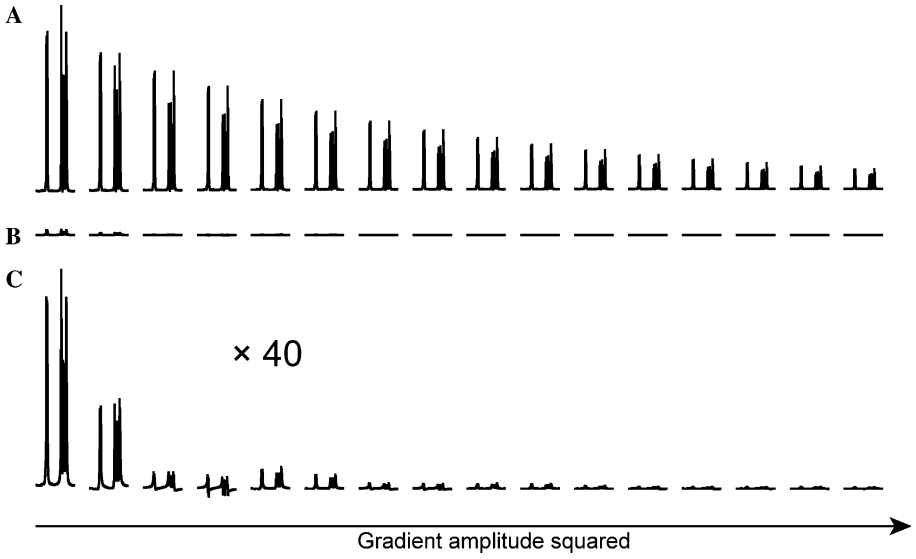

Fig. 3. Aromatic signals from quinine (7.1–7.6 ppm) in sample 1 as a function of increasing gradient strength. (A) Acquired with the PFGDSTE sequence (Fig. 1F); (B) acquired with the oneshot sequence (Fig. 1E)—same vertical scale as (A); (C) same as (B) but scaled up 40 times.

lays are unbalanced is indicative of coherent motion. Such an experiment can in principle be used to deduce the spectrum of flow velocities [40], but for a routine test for the presence or absence of convection it is generally sufficient simply to compare the signal amplitudes obtained with $\Delta_1 = \Delta_2$ and $\Delta_1 \gg \Delta_2$.

At room temperature, as expected, no evidence for convection is seen. On raising the nominal sample temperature by just one degree to 21 °C, however, a slight attenuation of the signal with imbalanced pulses can be seen, indicating that the system is just starting to convect. At 23 °C, convection is evident, increasing for 25

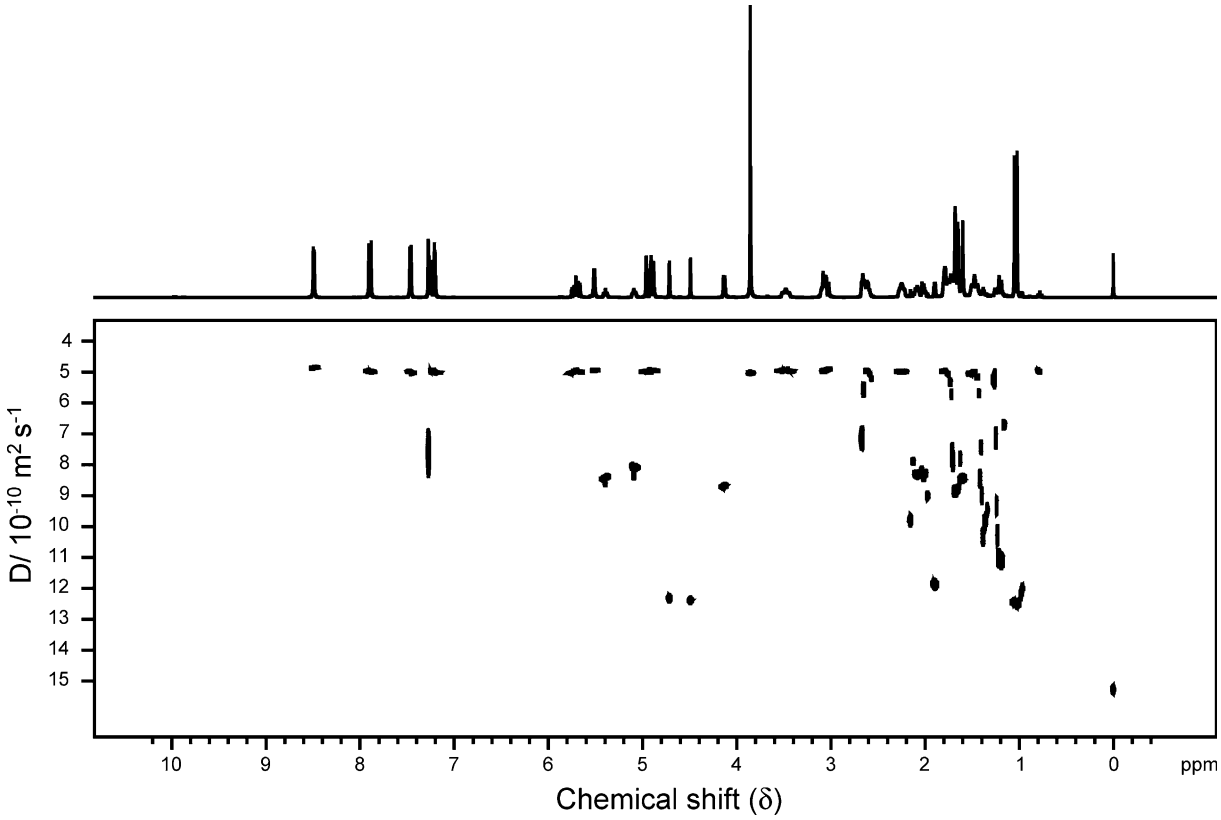

Fig. 4. 2D-DOSY spectrum of a mixture of camphene, geraniol, and quinine acquired with the convection compensated PFGDSTE sequence of Fig. 1F, with (top) the least attenuated proton spectrum.

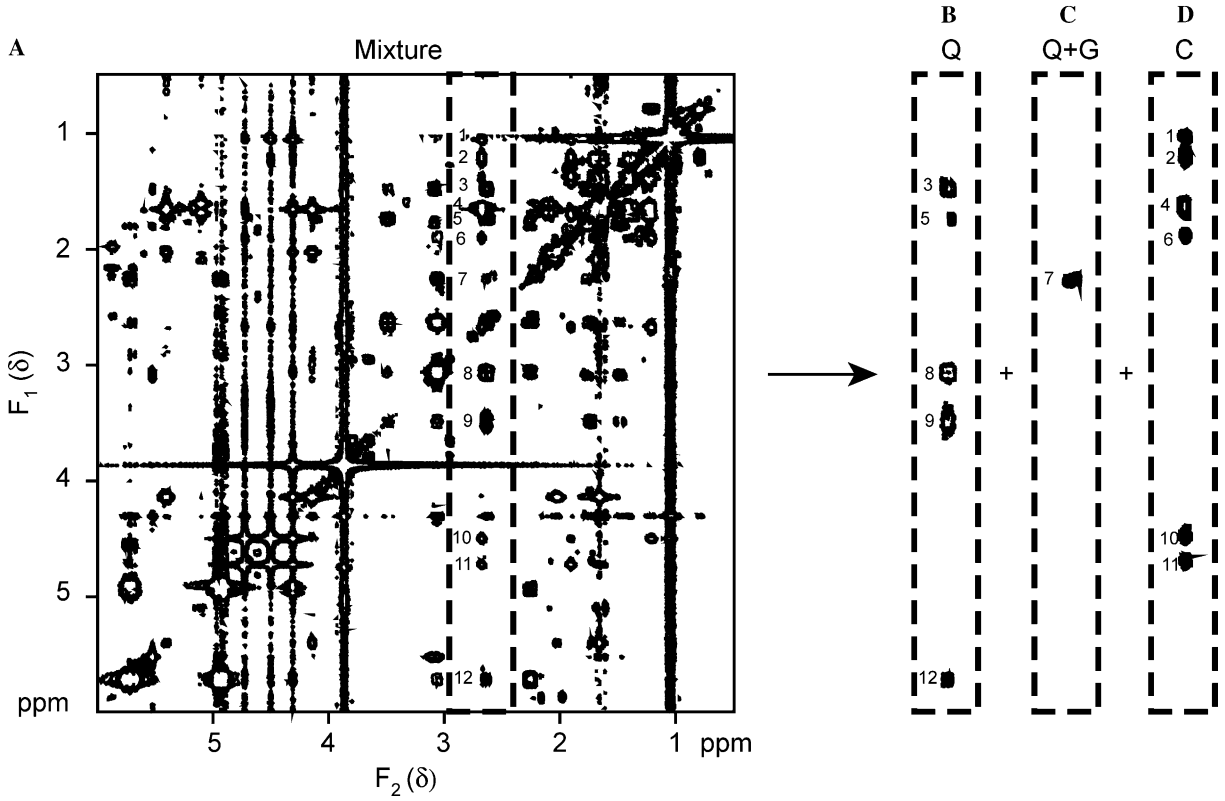

Fig. 5. COSY-IDOSY data acquired with the convection compensated sequence of Fig. 1B. (A) COSY spectrum for the lowest gradient amplitude—DOSY analysis was performed on cross peaks 1–12 as marked in the highlighted area; (B) projection onto the COSY plane for the diffusion region between 11 and 13×10^{-10} m^2 s^{-1}, containing signals from quinine (Q); (C) projection ranging from 7 to 9×10^{-10} m^2 s^{-1}, containing signals from quinine and geraniol (Q + G); (D) projection ranging from 4 to 6×10^{-10} m^2 s^{-1}, containing signals from camphene (C).

and 27 °C. Based on these data 25 °C was chosen as the temperature at which to test the effects of convection on the compensated sequences for sample 1. For sample 2 (in D_2O, a more viscous solvent), convection did not occur until higher temperature, so here 37 °C was chosen.

The detrimental effects of convection on the signal decay as a function of increasing gradient amplitude can be seen in Fig. 3, showing the decay of the aromatic signals of quinine between 7.1 and 7.6 ppm in sample 1. The data of Fig. 3E were acquired using the convection-compensated PFGDSTE sequence of Fig. 1F, and show the expected diffusional attenuation. In contrast, Fig. 3B, from the uncompensated oneshot sequence of Fig. 1E, shows the very much weaker signals and rapid attenuation caused by convection. The vertical expansion of the latter data in Fig. 3C shows that the signals undergo significant phase modulation, suggesting that the spins in the upward and downward flows may couple unequally to the receiver coil. The effects of convection here are florid and characteristic, but in cases of mild convection the only apparent effect is a slight increase in the diffusion coefficients obtained by fitting the peak decays. Here, it can be very useful to include a small amount of a high polymer as a reference signal: an increase in the apparent diffusion coefficient for such a signal is a sensitive indicator of problems such as convection.

A DOSY spectrum of sample 1, acquired with the PFGDSTE sequence, is shown in Fig. 4. As demonstrated above, the sample was convecting strongly, but, thanks to the convection compensation, the DOSY spectrum is still of high quality, and where there is no signal overlap the separation of the three components in the diffusion dimension is good. In contrast, the same experiment carried out with the oneshot sequence [45] did not produce any usable data.

Even the high quality DOSY spectrum of Fig. 4 does not resolve all the signals in the diffusion dimension, because of the signal overlap in the spectral dimension. The strategy of extending the DOSY experiment to three dimensions has recently been shown to be successful in separating the signals of a mixture of medium-chain alcohols using the COSY-IDOSY [21] (Fig. 1A) and 2DJ-IDOSY [20] experiments (Fig. 1C). As discussed above, these experiments lend themselves well to the inclusion of convection compensation (Figs. 1B and D).

COSY-IDOSY data were acquired for sample 1, with and without convection compensation. As expected, the rapid convection rendered the uncompensated experiment useless. The compensated experiment pro-

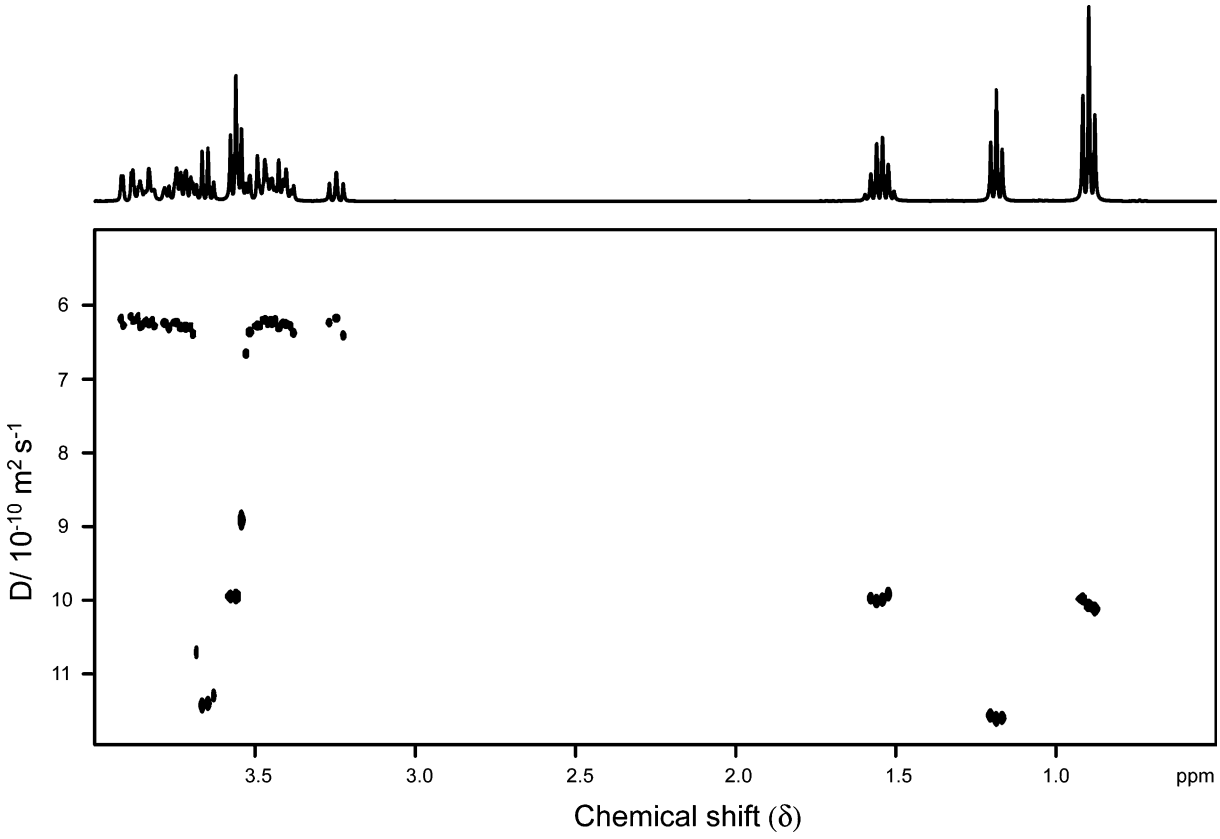

Fig. 6. Partial 2D-DOSY spectrum from 0.5 to 4.0 ppm of a mixture of glucose, 1-propanol and ethanol in D_2O (sample 2) acquired with the convection compensated the PFGDSTE sequence of Fig. 1F with (top) the least attenuated spectrum.

duced high quality data, as demonstrated by the 3D COSY-IDOSY results in Fig. 5. The overlapping signals at around 2.7 ppm in the conventional spectrum are now spread out in two dimensions, as seen in the least attenuated COSY spectrum drawn from the 3D-COSY-IDOSY dataset (Fig. 5A). In Figs. 5B–D

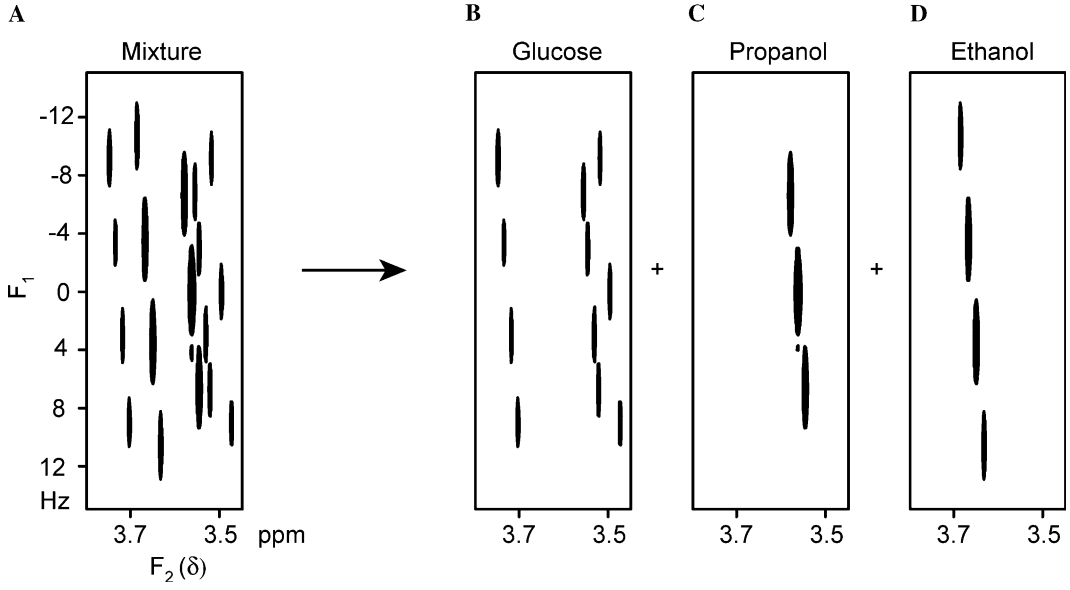

Fig. 7. 2DJ-IDOSY data for sample 2 acquired with the convection compensated sequence of Fig. 1D. (A) 2DJ spectrum for the lowest gradient amplitude—DOSY analysis was performed on all peaks; (B) projection onto the 2DJ spectrum plane of the diffusion region from 6.5 to 7.2×10^{-10} m^2 s^{-1}, containing the signals from glucose; (C) projection of the diffusion range 10.3 to 10.7×10^{-10} m^2 s^{-1}, containing the signals from 1-propanol; (D) projection of the diffusion range 12.0 to 12.7×10^{-10} m^2 s^{-1}containing the signals from ethanol.

three excerpts are shown from 3D-projections onto the COSY plane for different diffusion ranges of the 3D-COSY-IDOSY spectrum, containing the peaks from camphene, geraniol and quinine. Just one cross-peak, no 7, is unresolved in the COSY spectrum and contains signals from two components (quinine and geraniol).

The convection compensation of 2DJ-IDOSY is demonstrated for the overlapping signals around 3.6 ppm, in sample 2. In the 2D-DOSY spectrum (Fig. 6), these signals are not resolved in either dimension. In the 2DJ spectrum they are resolved into two doublets of doublets and a triplet originating from glucose, a triplet from 1-propanol, and a quartet from ethanol, which are well-separated in the diffusion dimension of the 3D 2DJ-IDOSY spectrum of Fig. 7. Recording the same experiment using the normal, uncompensated, 2DJ-IDOSY sequence did not result in usable data at this temperature.

6. Conclusions

Convection can cause grave problems when trying to determine diffusion coefficients using PFG-NMR experiments. Convection-compensated pulse sequences can be a convenient and effective way of dealing with the problem. In many experiments, the compensation can be included with little or no loss of signal-to-noise ratio. This has been demonstrated for two 3D-DOSY experiments of the IDOSY family: 2DJ-IDOSY and COSY-IDOSY.

Acknowledgment

Support from the Engineering and Physical Sciences Research Council (Grant ref GR/S90751/01) is gratefully acknowledged.

References

[1] B. Antalek, Using pulsed gradient spin echo NMR for chemical mixture analysis: how to obtain optimum results, Concept Magn. Reson. 14 (2002) 225–258.
[2] C.S. Johnson, Diffusion ordered nuclear magnetic resonance spectroscopy: principles and applications, Prog. Nucl. Magn. Reson. Spectros. 34 (1999) 203–256.
[3] G.A. Morris, in: D.M. Grant, R.K. Harris (Eds.), Encyclopedia of Nuclear Magnetic Resonance, John Wiley, Chichester, 2002, pp. 35–44.
[4] H. Barjat, G.A. Morris, S. Smart, A.G. Swanson, S.C.R. Williams, High-resolution diffusion-ordered 2D spectroscopy (HR-Dosy)—a new tool for the analysis of complex-mixtures, J. Magn. Reson. B 108 (1995) 170–172.
[5] A.A. Istratov, O.F. Vyvenko, Exponential analysis in physical phenomena, Rev. Sci. Instrum. 70 (1999) 1233–1257.
[6] L. Ambrosone, A. Ceglie, G. Colafemmina, G. Palazzo, Resolving complex mixtures by means of pulsed gradient spin–echo NMR experiments, Phys. Chem. Chem. Phys. 4 (2002) 3040–3047.
[7] M.A. Delsuc, T.E. Malliavin, Maximum entropy processing of DOSY NMR spectra, Anal. Chem. 70 (1998) 2146–2148.
[8] K.F. Morris, C.S. Johnson, Resolution of discrete and continuous molecular-size distributions by means of diffusion-ordered 2D NMR-spectroscopy, J. Am. Chem. Soc. 115 (1993) 4291–4299.
[9] G.S. Armstrong, N.M. Loening, J.E. Curtis, A.J. Shaka, V.A. Mandelshtam, Processing DOSY spectra using the regularized resolvent transform, J. Magn. Reson. 163 (2003) 139–148.
[10] R. Huo, R. Wehrens, L.M.C. Buydens, Improved DOSY NMR data processing by data enhancement and combination of multivariate curve resolution with non-linear least square fitting, J. Magn. Reson. 169 (2004) 257–269.
[11] R. Huo, R. Wehrens, J. van Duynhoven, L.M.C. Buydens, Assessment of techniques for DOSY NMR data processing, Anal. Chim. Acta 490 (2003) 231–251.
[12] P. Stilbs, K. Paulsen, P.C. Griffiths, Global least-squares analysis of large, correlated spectral data sets: Application to component-resolved FT-PGSE NMR spectroscopy, J. Phys. Chem. 100 (1996) 8180–8189.
[13] L.C.M. Van Gorkom, T.M. Hancewicz, Analysis of DOSY and GPC-NMR experiments on polymers by multivariate curve resolution, J. Magn. Reson. 130 (1998) 125–130.
[14] W. Windig, B. Antalek, Direct exponential curve resolution algorithm (DECRA): a novel application of the generalized rank annihilation method for a single spectral mixture data set with exponentially decaying contribution profiles, Chemometr. Intell. Lab. 37 (1997) 241–254.
[15] H. Barjat, G.A. Morris, A.G. Swanson, A three-dimensional DOSY-HMQC experiment for the high- resolution analysis of complex mixtures, J. Magn. Reson. 131 (1998) 131–138.
[16] N. Birlirakis, E. Guittet, A new approach in the use of gradients for size-resolved 2D-NMR experiments, J. Am. Chem. Soc. 118 (1996) 13083–13084.
[17] E.K. Gozansky, D.G. Gorenstein, Dosy-Noesy: diffusion-ordered Noesy, J. Magn. Reson. B 111 (1996) 94–96.
[18] M.F. Lin, M.J. Shapiro, Mixture analysis in combinatorial chemistry. Application of diffusion-resolved NMR spectroscopy, J. Org. Chem. 61 (1996) 7617–7619.
[19] L.H. Lucas, W.H. Otto, C.K. Larive, The 2D-J-DOSY experiment: resolving diffusion coefficients in mixtures, J. Magn. Reson. 156 (2002) 138–145.
[20] M. Nilsson, A.M. Gil, I. Delgadillo, G.A. Morris, Improving pulse sequences for 3D diffusion-ordered NMR spectroscopy: 2DJ-IDOSY, Anal. Chem. 76 (2004) 5418–5422.
[21] M. Nilsson, A.M. Gil, I. Delgadillo, G.A. Morris, Improving pulse sequences for 3D DOSY: COSY-IDOSY, Chem. Commun. (2005) 1737–1739.
[22] M.J. Stchedroff, A.M. Kenwright, G.A. Morris, M. Nilsson, R.K. Harris, 2D and 3D DOSY methods for studying mixtures of oligomeric dimethylsiloxanes, Phys. Chem. Chem. Phys. 6 (2004) 3221–3227.
[23] R.T. Williamson, E.L. Chapin, A.W. Carr, J.R. Gilbert, P.R. Graupner, P. Lewer, P. McKamey, J.R. Carney, W.H. Gerwick, New diffusion-edited NMR experiments to expedite the dereplication of known compounds from natural product mixtures, Org. Lett. 2 (2000) 289–292.
[24] D.H. Wu, A.D. Chen, C.S. Johnson, Heteronuclear-detected diffusion-ordered NMR spectroscopy through coherence transfer, J. Magn. Reson. A 123 (1996) 215–218.
[25] D.H. Wu, A.D. Chen, C.S. Johnson, Three-dimensional diffusion-ordered NMR spectroscopy: the homonuclear COSY–DOSY experiment, J. Magn. Reson. A 121 (1996) 88–91.
[26] D.H. Wu, W.S. Woodward, C.S. Johnson, A sample spinner for vibration-sensitive liquid-state experiments with application to

diffusion-ordered 2D NMR, J. Magn. Reson. A 104 (1993) 231–233.
[27] N. Hedin, I. Furo, Temperature imaging by H-1 NMR and suppression of convection in NMR probes, J. Magn. Reson. 131 (1998) 126–130.
[28] A. Jerschow, N. Müller, Suppression of convection artifacts in stimulated-echo diffusion experiments. Double-stimulated-echo experiments, J. Magn. Reson. 125 (1997) 372–375.
[29] N. Hedin, T.Y. Yu, I. Furo, Growth of C12E8 micelles with increasing temperature. A convection-compensated PGSE NMR study, Langmuir 16 (2000) 7548–7550.
[30] A. Jerschow, Thermal convection currents in NMR: Flow profiles and implications for coherence pathway selection, J. Magn. Reson. 145 (2000) 125–131.
[31] G.H. Sørland, J.G. Seland, J. Krane, H.W. Anthonsen, Improved convection compensating pulsed field gradient spin–echo and stimulated-echo methods, J. Magn. Reson. 142 (2000) 323–325.
[32] W.J. Goux, L.A. Verkruyse, S.J. Salter, The impact of Rayleigh–Benard convection on NMR pulsed-field-gradient diffusion measurements, J. Magn. Reson. 88 (1990) 609–614.
[33] E. Martinez-Viviente, P.S. Pregosin, Low temperature H-1-, F-19-, and P-31-PGSE diffusion measurements. Applications to cationic alcohol complexes, Helv. Chim. Acta 86 (2003) 2364–2378.
[34] M.L. Tillett, L.Y. Lian, T.J. Norwood, Practical aspects of the measurement of the diffusion of proteins in aqueous solution, J. Magn. Reson. 133 (1998) 379–384.
[35] K. Hayamizu, W.S. Price, A new type of sample tube for reducing convection effects in PGSE-NMR measurements of self-diffusion coefficients of liquid samples, J. Magn. Reson. 167 (2004) 328–333.
[36] N. Esturau, F. Sanchez-Ferrando, J.A. Gavin, C. Roumestand, M.A. Delsuc, T. Parella, The use of sample rotation for minimizing convection effects in self-diffusion NMR measurements, J. Magn. Reson. 153 (2001) 48–55.
[37] J. Lounila, K. Oikarinen, P. Ingman, J. Jokisaari, Effects of thermal convection on NMR and their elimination by sample rotation, J. Magn. Reson. A 118 (1996) 50–54.
[38] A. Allerhand, R.E. Addleman, D. Osman, Ultrahigh resolution NMR.1. General-considerations and preliminary-results for C-13 NMR, J. Am. Chem. Soc. 107 (1985) 5809–5810.
[39] N.M. Loening, J. Keeler, Temperature accuracy and temperature gradients in solution- state NMR spectrometers, J. Magn. Reson. 159 (2002) 55–61.
[40] N.M. Loening, J. Keeler, Measurement of convection and temperature profiles in liquid samples, J. Magn. Reson. 139 (1999) 334–341.
[41] N. Boden, S.A. Corne, P. Halfordmaw, D. Fogarty, K.W. Jolley, Sample cell for high-precision temperature-dependence NMR experiments, J. Magn. Reson. 98 (1992) 92–108.
[42] A. Jerschow, N. Müller, 3D diffusion-ordered TOCSY for slowly diffusing molecules, J. Magn. Reson. A 123 (1996) 222–225.
[43] K.I. Momot, P.W. Kuchel, Convection-compensating PGSE experiment incorporating excitation-sculpting water suppression (CONVEX), J. Magn. Reson. 169 (2004) 92–101.
[44] A. Jerschow, N. Müller, Convection compensation in gradient enhanced nuclear magnetic resonance spectroscopy, J. Magn. Reson. 132 (1998) 13–18.
[45] M.D. Pelta, G.A. Morris, M.J. Stchedroff, S.J. Hammond, A one-shot sequence for high-resolution diffusion-ordered spectroscopy, Magn. Reson. Chem. 40 (2002) S147–S152.